

Application of high performance one-dimensional chaotic map in key expansion algorithm

Yuxuan Li (✉ liyux2001@163.com)

University of Jinan

Research Article

Keywords: Chaotic map, Lyapunov Exponent, Key expansion algorithm

Posted Date: June 22nd, 2023

DOI: <https://doi.org/10.21203/rs.3.rs-3091298/v1>

License:  This work is licensed under a Creative Commons Attribution 4.0 International License.

[Read Full License](#)

Additional Declarations: No competing interests reported.

1 **Application of high performance one-dimensional chaotic map in key**
2 **expansion algorithm**

3 **Yuxuan Li**¹✉

4 ¹ School of Mathematical Sciences, University of Jinan, Jinan, China

5 ✉ Corresponding author liyux2001@163.com

6 **Abstract**

7 In this paper, we present a key expansion algorithm based on a high-performance one-dimensional
8 chaotic map. Traditional one-dimensional chaotic maps exhibit several limitations, prompting us
9 to construct a new map that overcomes these shortcomings. By analyzing the structural
10 characteristics of classic 1D chaotic maps, we propose a high-performance 1D map that
11 outperforms multidimensional maps introduced by numerous researchers in recent years.

12 In block cryptosystems, the security of round keys is of utmost importance. To ensure the
13 generation of secure round keys, a sufficiently robust key expansion algorithm is required. The
14 security of round keys is assessed based on statistical independence and sensitivity to the initial
15 key. Leveraging the properties of our constructed high-performance chaotic map, we introduce a
16 chaotic key expansion algorithm.

17 Our experimental results validate the robust security of our proposed key expansion algorithm,
18 demonstrating its resilience against various attacks. The algorithm exhibits strong statistical
19 independence and sensitivity to the initial key, further strengthening the security of the generated
20 round keys.

21 **Keywords** Chaotic map · Lyapunov Exponent · Key expansion algorithm

22 **1 Introduction**

23 With the rapid advancement of information technology, the significance of information security
24 has garnered increasing attention, consequently driving the progress of cryptography. Among
25 various encryption techniques, block ciphers hold a crucial position. In 2000, the Advanced
26 Encryption Standard (AES) emerged as a pivotal block cipher. The AES encryption algorithm
27 consists of multiple encryption rounds, where each round involves XOR operations between round
28 keys and encryption blocks [1].

29 Chaos is renowned for its sensitivity to initial values and the unpredictable nature of the
30 sequences it generates [2,3]. In recent years, chaotic maps have found extensive applications in the
31 realm of encryption [4-12]. However, traditional low-dimensional chaotic systems exhibit certain
32 shortcomings in cryptographic applications, such as discontinuous chaotic intervals and
33 predictable chaotic signals. To address these issues, researchers have proposed high-dimensional
34 chaotic maps [13-16]. Although higher dimensions result in more complex mapping forms, they
35 also increase computational requirements. Consequently, we draw inspiration from these
36 developments and aim to design a high-performance one-dimensional chaotic map with a simple
37 structure.

38 In a block cipher algorithm, apart from round key addition, all other steps do not utilize keys.
39 This implies that an attacker could calculate the inverse without possessing the key, underscoring
40 the pivotal role of the round key in ensuring the security of the block cipher. The round key is
41 derived from a key expansion algorithm, thus emphasizing the significance of devising a secure
42 key expansion algorithm. Upon analyzing the key expansion algorithm employed by AES, we

43 observe that it undergoes a reversible serial transformation process. If the round key for any round
44 is known, one can deduce the round key for other rounds or even the initial key. This substantially
45 diminishes the security of block ciphers and exposes vulnerabilities to side-channel attacks and
46 other forms of intrusion. Inspired by the successful applications of chaotic maps in various
47 cryptographic domains, we propose leveraging chaotic maps to generate a more secure key
48 expansion algorithm.

49 In this study, we introduce a high-performance 1D chaotic map tailored for our key expansion
50 algorithm, drawing insights from the analysis of various classical 1D chaotic map structures. By
51 examining the nonlinear dynamics inherent in our mapping, we showcase its superiority over
52 alternative maps. Subsequently, we put forth a chaotic key expansion algorithm built upon this
53 chaotic map, accompanied by a thorough security analysis.

54 The subsequent sections of this paper are organized as follows: Section 2 provides an analysis
55 of several well-established classical 1D chaotic maps. In Section 3, we present our high-
56 performance 1D chaotic map, along with an examination of its Lyapunov Exponent and K-Entropy.
57 Section 4 introduces our chaotic key expansion algorithm, while addressing its security
58 considerations. Finally, Section 5 concludes this paper, summarizing the key findings and
59 contributions.

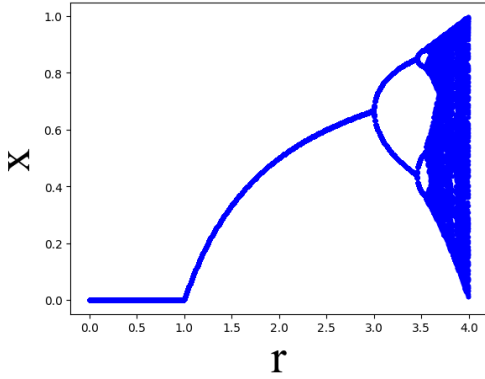
60 **2 Classic 1D chaotic maps**

61 **2.1 Logistic map**

62 The Logistic map represents a classical 1D chaotic map, which can be mathematically
63 expressed by Eq. (1) [17].

64
$$x(i+1) = rx(i)(1-x(i)), \tag{1}$$

65 where $x \in [0,1]$ is the state variable and $r \in [0,4]$ is the control parameter. Its bifurcation
 66 diagram is shown in Fig. 1. When $r \in [3.56995,4]$, the system enters a chaotic state [17].



67
 68 **Fig. 1** Bifurcation diagram of the Logistic map

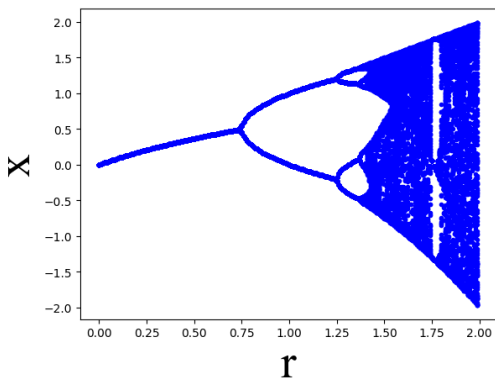
69 **2.2 Quadratic map**

70 The Quadratic map can be mathematically represented by Eq. (2) [18].

71
$$x(i+1) = r - x(i)^2, \tag{2}$$

72 where $x \in [-2,2]$ is the state variable and $r \in [0,2]$ is the control parameter. The bifurcation
 73 diagram of the Quadratic map is depicted in Fig. 2.

74



75

76 **Fig. 2** Bifurcation diagram of the Quadratic map

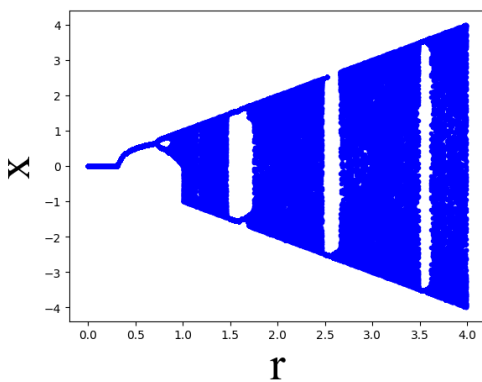
77 **2.3 Sine map**

78 In addition, we introduce another classical one-dimensional map, known as the Sine map. The Sine
79 map can be mathematically represented by Eq. (3) [19].

$$80 \quad x(i+1) = r \sin(\pi x(i)), \quad (3)$$

81 where $x \in [-4, 4]$ is the state variable and $r \in [0, 4]$ is the control parameter. The bifurcation
82 diagram of the Sine map is depicted in Fig. 3.

83



84

85 **Fig. 3** Bifurcation diagram of the Sine map

86 **3 The proposal of efficient 1D chaotic map and performance evaluations**

87 Upon examining the limitations of the previously introduced classical 1D chaotic maps, it becomes
88 evident that they share common weaknesses, such as discontinuities in the chaotic interval. These
89 maps may exhibit non-chaotic phenomena, including fixed points, at certain control parameter
90 values. Consequently, the predictability of chaotic signals restricts their applicability in
91 cryptography. Our objective is to overcome these limitations without increasing the dimensionality

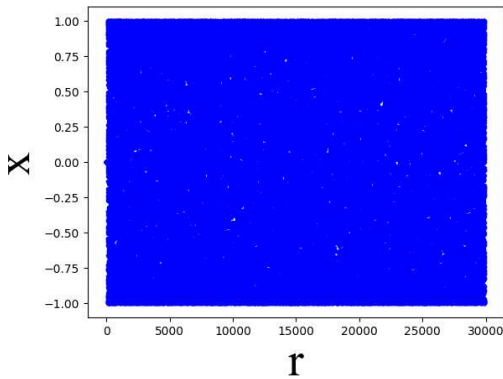
92 of the map.

93 We embark on improving the structure of the existing 1D map by leveraging the inherent
94 characteristics of nonlinear components. Chaos, as a typical nonlinear phenomenon in iterative
95 maps, necessitates the presence of nonlinear components that eliminate the superposition effect.
96 The sine map, a classical nonlinear component, effectively constrains the range of state variables.
97 Additionally, the tangent map displays exceptional sensitivity to changes in initial values within
98 specific ranges, making it an ideal candidate for constructing chaotic maps.

99 By amalgamating these existing structures and incorporating both the sine map and the tangent
100 map, we propose a high-performance 1D chaotic map, mathematically expressed by Eq. (4).

101
$$x(i+1) = \sin(\tan(r^2(r - x(i)^2))), \quad (4)$$

102 where $x \in [-1,1]$ is the state variable and $r \in [0, 3 \times 10^4]$ is the control parameter. We have
103 named this new chaotic map the 1D-sin-tan-quadratic chaotic map (1D-STQCM). The bifurcation
104 diagram of the 1D-STQCM is presented in Fig. 4, demonstrating its ability to exhibit chaos across
105 a significantly wider parameter range. In the subsequent analysis, we delve into the dynamical
106 performance of the 1D-STQCM, evaluating its key characteristics and properties.



107
108 **Fig. 4** Bifurcation diagram of 1D-STQCM

109 **3.1 Lyapunov Exponent**

110 The Lyapunov Exponent serves as a crucial index for describing the stability and chaotic properties
111 of dynamical systems. It quantifies the rate at which adjacent orbits in phase space diverge, thus
112 capturing the system's sensitive dependence. This measure is commonly employed to analyze
113 nonlinear dynamical systems, particularly those exhibiting chaotic behavior [20]. Chaotic systems
114 display a high degree of sensitivity to initial conditions, where small perturbations can lead to
115 significant deviations in system behavior. The Lyapunov Exponent effectively captures this
116 sensitive dependence and provides insights into the stability and chaotic nature of the system.

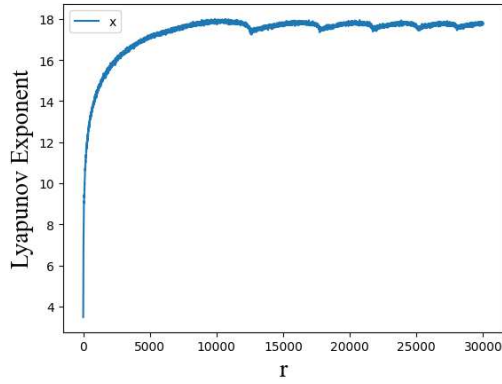
117 Typically, the Lyapunov Exponent is expressed as a real number or a set of real numbers. Each
118 index corresponds to a specific direction within the system, describing the rate of separation along
119 that particular direction. A positive Lyapunov Exponent indicates exponential divergence between
120 adjacent orbits, indicating chaotic behavior. Conversely, a negative Lyapunov Exponent suggests
121 exponential convergence between adjacent orbits, indicating stability. A Lyapunov Exponent of
122 zero signifies linear separation or convergence, indicating bounded behavior within the system.

123 It is worth noting that the Lyapunov Exponent is a statistical measure that is not sensitive to
124 the specific evolution path of the system. It is typically obtained by calculating an average value
125 and can be estimated using numerical simulation or mathematical analysis methods. In other words,
126 a larger positive Lyapunov Exponent indicates a more pronounced chaotic performance. Ref. [21]
127 provides a method for computing the Lyapunov Exponent, expressed by Eq (5).

$$128 \quad LE = \lim_{x \rightarrow \infty} \frac{1}{n} \sum_{i=0}^{n-1} \ln |f'(x_i)|, \quad (5)$$

129 where LE denotes the Lyapunov Exponent and $f(x_i)$ is the time series of length n generated
130 by the chaotic system. The curve illustrating the Lyapunov Exponent of the 1D-STQCM in relation
131 to the control parameter is presented in Fig. 5. Furthermore, a comparison between the maximum
132 Lyapunov Exponent of the 1D-STQCM and other chaotic maps is presented in Table 1. Notably,

133 despite being one-dimensional, the dynamic performance of the 1D-STQCM surpasses that of
 134 more recent three-dimensional maps, as evident from the table.



135
 136 **Fig. 5** Lyapunov Exponent of 1D-STQCM

137 **Table 1** A comparison of the maximum K-Entropy and maximum Lyapunov Exponents of 1D-
 138 STQCM with other maps.

Map	Max Lyapunov Exponent	Max K-Entropy
Logistic map	0.6929	0.3456
Quadratic map	0.7025	0.2876
Sine map	0.6919	0.3791
ICQM [22]	15.2462	0.8862
EQM [23]	16.6540	1.4343
3D-ICQM [24]	17.1231	0.6893
3D-ECM [25]	16.9166	0.9238
1D-STQCM	17.9990	1.4440

139
 140 **3.2 K-Entropy**

141 In discrete chaotic systems, K-Entropy serves as a vital concept for measuring the complexity and
 142 uncertainty inherent in the system. It stems from the notion of entropy, which is a fundamental
 143 concept in information theory used to quantify the uncertainty of random variables. In the context
 144 of discrete random variables, entropy describes the average amount of information present. In
 145 discrete chaotic systems, K-Entropy extends the concept of entropy to discrete variable sequences.
 146 It characterizes the rate at which information grows during the dynamic evolution of discrete
 147 chaotic systems.

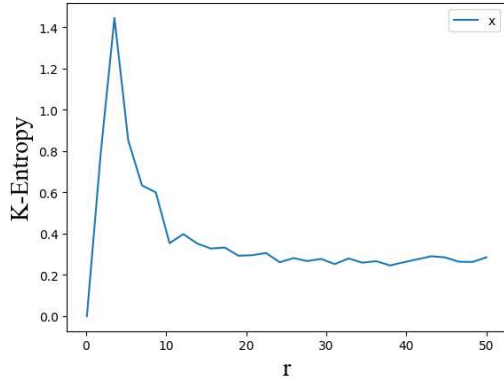
148 The calculation method for K-Entropy involves dividing the state sequence of the system into
 149 different subsequences of length K . Subsequently, the entropy of each subsequence is computed,
 150 and the average of these entropies is determined. This average reflects the overall rate of
 151 information growth within the system. The value of K-Entropy is typically directly linked to the
 152 complexity and chaotic nature of the system. In a simple periodic system, the K-Entropy value
 153 may be low as the entropy of the sequence tends to remain stable. However, in a chaotic system,
 154 characterized by high sensitivity and uncertainty, the K-Entropy value tends to be higher due to
 155 the rapid increase in sequence entropy.

156 Ref. [26] provides a method for calculating K-Entropy, as expressed in Eq. (6).

$$157 \quad KE = -\lim_{\tau \rightarrow 0} \lim_{\varepsilon \rightarrow 0} \lim_{n \rightarrow \infty} \frac{1}{n\tau} \sum_{i_1, i_2, \dots, i_n} p(i_1, i_2, \dots, i_n) \ln(p(i_1, i_2, \dots, i_n)), \quad (6)$$

158 where n is the embedding dimension, τ denotes the time delay, p is the joint probability.

159 The K-Entropy of the 1D-STQCM is illustrated in Fig. 6, revealing that with the appropriate
 160 selection of control parameters, our map exhibits a significantly high K-Entropy. This
 161 characteristic renders the generated chaotic sequence highly unpredictable. The superiority of the
 162 1D-STQCM in terms of K-Entropy is also demonstrated in Table 1, further highlighting its
 163 advantages over other chaotic maps.



164

165 **Fig. 6** K-Entropy of 1D-STQCM

166 **4 Key expansion algorithm based on 1D-STQCM and its security analysis**

167 **4.1 Proposed key expansion algorithm**

168 Our proposed key expansion algorithm targets the AES encryption algorithm structure with a key
 169 length of 128 bits, which encrypts the block for 10 rounds, so our key expansion algorithm will
 170 produce 10 round keys with a length of 128 bits. For other structures of block ciphers, the
 171 corresponding key expansion algorithm can be obtained by making simple changes. Before
 172 presenting the algorithm, we first make some notational conventions. We agree that a word is 4
 173 bytes, that is, 32 bits, and use the array $IK[0:3]$ to represent the initial key of 4 words, and the
 174 array $w[0:43]$ to represent the 11 keys including the initial key and the 10 round keys of 44
 175 words. Both initial and round keys are expressed in hexadecimal. Our proposed key expansion
 176 algorithm is denoted by Algorithm 1. We need computers with high floating-point precision to
 177 better exploit the performance of 1D-STQCM and thus obtain better properties in key expansion.

178 **Algorithm 1:** Key expansion Algorithm based on 1D-STQCM

179 **Input:** $IK[0:3]$.

180 **Output:** $w[0:43]$.

181 **Initial:**

```

182   Let  $x[0:3]=IK[0:3]$ ;
183   Set  $w[0:3]=IK[0:3]$ ;
184   Set control parameter  $r = \max(\text{hex2dec}(w[0]),5)$ , 1D-STQCM uses this control parameter.
185   if  $w[0] \oplus w[1] \oplus w[2] \oplus w[3] = \text{all zeros}$  do:
186        $w[0] = w[0] \oplus 36118107$  // Any number that can eliminate the symmetry will do.
187   end if
188   for  $i=0, 1, 2, 3$  do:
189        $x[i] = \frac{\text{hex2dec}(x[i])}{16^8 - 1}$ ;
190   end for
191   for  $i=1, \dots, 100$  do:
192       for  $j=0, \dots, 3$  do:
193            $x[j] = \text{1D-STQCM}(x[j])$ ;
194       end for
195   end for
196
197   for  $i=4, \dots, 43$  do:
198       for  $j=0, \dots, 3$  do:
199            $x[j] = \text{1D-STQCM}(x[j])$ 
200       end for
201        $temp = x$ ;
202       for  $j=0, \dots, 3$  do:
203            $temp[j] = \text{dec2hex}(10^{16} \times x[j] \bmod 16^8)$ 
204       end for
205       The bitwise XOR operation of the components of  $temp$  assigns the result to  $w[i]$ ;
206   end for
207   Output  $w$ 

```

208

 Given an initial key, the result of a key expansion is shown in Table 2. Then we analyze the
209 security of the proposed key expansion algorithm.

210 **Table 2** An instance of key expansion using our algorithm.

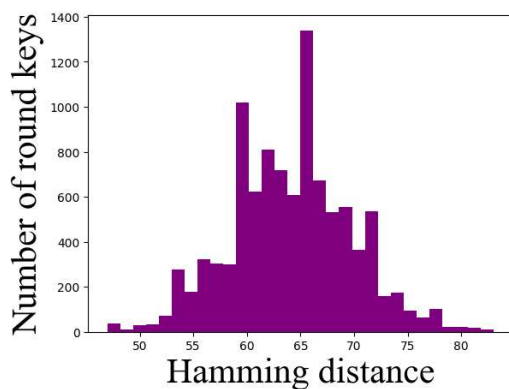
Round	Round Key
0(Initial key)	0F1571C947D9E8590CB7ADD6AF7F6798
1	7E65712BD13C4285394244BF3CD8CD6A
2	6CBA147DC3B2589D2F295666DAD889C6
3	A7E1DDD08BC2C60133BE18EC73E3F520
4	71B47C1D4E443387BCA43F77EF2C3B24

5	31E3C53F7AF4C192AE6AC7158964CB1B
6	DBDA0082A00868D6604088EBEDE96A55
7	049DCCED770C74A74EA5BE07E8C4B0CA
8	64410DFEE40BCAF9C87E1AE0708E5F46
9	0038AC193043977FB89955FF4EB2749A
10	AD7E9A30FDE653E59C96AD3735F8B38E

211

212 **4.1 Independence of the round key**

213 To verify the independence of the round key, we need to calculate the number of bit change rate
 214 (NBCR). The ideal value of NBCR is 50%, meaning that the round key is independent [27]. To
 215 compute NBCR we first compute the Hamming distance, since NBCR is equal to the Hamming
 216 distance of two sequences divided by the bit length of the sequence. The Hamming distance
 217 between two sequences is defined as different bits in binary. We generated 10,000 round keys from
 218 an initial key according to our algorithm, counted the Hamming distance between these round keys
 219 and the initial key, and drew the histogram as shown in Fig. 7.



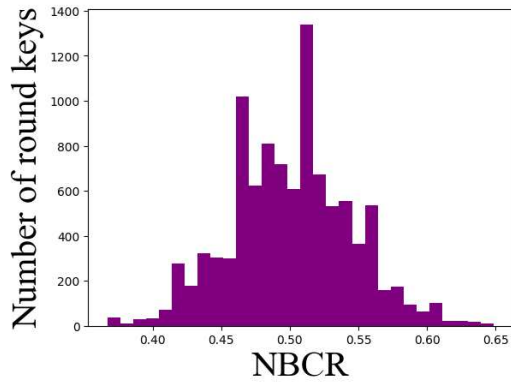
220

221 **Fig. 7** Distribution of Hamming distance between 10000 round keys and the initial key.

222 The Hamming distance divided by the key length, that is, divided by 128 bits, yields the NBCR.

223 Naturally we can plot the NBCR distribution of 10000 round keys as shown in Fig. 8. It can be

224 seen that the NBCR of round keys is close to the ideal value of 50%, which indicates that round
 225 keys are independent.



226
 227 **Fig. 8** Distribution of NBCR of 10000 round keys.

228 **4.2 Strict avalanche criterion**

229 After testing the independence of the round key, we also need to test the sensitivity of the key
 230 expansion algorithm to the initial key, which manifests as a strict avalanche effect. A strict
 231 avalanche effect means that any bit of the initial key is reversed, with a 50% probability for every
 232 bit of the round key [28]. We reverse the 1 bit of the initial key in Table 2, apply the key expansion
 233 algorithm to obtain 10 round keys, and for each round, calculate the Hamming distance between
 234 the corresponding round keys, and the results are shown in Table 3. It can be seen that the
 235 Hamming distance between each pair of corresponding round keys is about half of the key length,
 236 indicating that our key expansion algorithm satisfies the strict avalanche effect, thus proving the
 237 sensitivity to the initial key.

238 **Table 3** Hamming distance between corresponding round keys.

Round	Value	Hamming distance
0(Initial key)	1F1571C947D9E8590CB7ADD6AF7F6798	1

1	36BB7A50B2A3171CE7DCAB909A932D62	70
2	D22D7D34E9B177315B55A3AAFF6F7233	73
3	5C1C3333FD2FEDE4337D554A627E201A	73
4	8AC50398B7B8CF5C59100F2F7D5B8A44	74
5	AD46D24D3417AA4C26ACE0569CCE0BD6	63
6	9657AD31928AF6BAC5C3BC19A9F43C03	61
7	650DBFF33F1CC53179C5B984E0121E8F	52
8	5C75A3B9344C8C96208B94E584DD1CA9	66
9	80910E3ACF17C565DDFE4F0460175354	64
10	31EA9CB8BA229F56E558A606E4F5C4DD	60

239 4.2 Diffusion and confusion analysis

240 The combination of confusion and diffusion is considered a fundamental element in achieving the
241 security of cryptographic algorithms. The effects of confusion and diffusion work together to
242 reinforce each other, making the security of cryptographic algorithms more robust. In key
243 expansion algorithms, diffusion can be understood as the idea that small changes in the initial key
244 can be spread out and mixed in the round key by distributing each bit of information in the initial
245 key to as many positions as possible. Based on previous experiments, our key expansion algorithm
246 is sensitive to the initial key and satisfies the diffusion effect.

247 Confusion, on the other hand, can be understood as creating a highly complex and
248 unpredictable relationship between the initial key and the round key, by making the relationship
249 between the initial key and the round key confusing and complicated. To implement the confusion
250 effect, we use highly unpredictable chaotic mapping in our key extension algorithm.

251 4.3 The ability to resist side channel attacks

252 A side-channel attack [29] is a method employed in cryptanalysis that utilizes the physical
253 information leakage arising from the execution of encryption operations by an encryption device,
254 rather than directly attempting to crack the encryption algorithm, in order to obtain sensitive
255 information. The fundamental concept behind a side-channel attack is that the internal state of the
256 encryption device exhibits various physical characteristics, such as changes in power consumption
257 and electromagnetic radiation, during the execution of encryption operations. These physical
258 characteristics are correlated with the device's internal operation process and data, which can be
259 monitored and recorded by specialized devices or sensors. By collecting a significant amount of
260 side-channel data, an attacker can employ statistical analysis, pattern recognition, and other
261 techniques to infer the round key utilized by the encryption algorithm.

262 Based on our previous analysis, the keys generated by our key expansion algorithm are
263 independent, and even if an attacker manages to obtain a round key, they cannot deduce the initial
264 key. Therefore, our key expansion algorithm effectively withstands side-channel attacks.

265 **4.4 Ability to resist differential attacks**

266 Differential attack is another commonly used method in cryptanalysis. It aims to obtain key
267 information, such as the key or plaintext, by analyzing the output differences of cryptographic
268 algorithms when subjected to different input differences [30]. The fundamental concept behind a
269 differential attack is to select a pair of input plaintexts with a small difference between them and
270 observe the resulting output difference during the algorithm's execution. By repeating this process
271 multiple times, collecting a large number of differential pairs, and performing counting and
272 analysis, an attacker can infer certain bits of the key or the internal state of the algorithm.

273 The key expansion algorithm satisfies the strict avalanche effect, and the change of initial

274 key does not cause the characteristic difference of round key, which can effectively resist
275 differential attacks.

276 **5 Conclusion**

277 In this study, we have proposed a high-performance 1D chaotic map, named 1D-STQCM. The
278 Lyapunov Exponent and K-Entropy tests conducted on 1D-STQCM have demonstrated its robust
279 performance. Furthermore, our key expansion algorithm generates round keys that exhibit
280 independence from the initial key and sensitivity to changes in the initial key. These characteristics
281 address the limitations found in many existing key expansion algorithms, including the AES key
282 expansion algorithm, and provide effective resistance against side-channel attacks and differential
283 attacks. In the future, the application of 1D-STQCM can be extended to various domains, such as
284 information encryption, random number generation, and the construction of strong S-boxes. The
285 versatility and security properties of 1D-STQCM make it a promising tool for enhancing security
286 measures in these areas.

287 **Data Availability** No data was used in this paper.

288 **Declarations** None.

289 **Conflict of interest** All authors have no relevant financial or non-financial interests to disclose.

290 **Ethical approval** All authors accept ethical responsibility.

291 **Inform consent** All the authors agreed to submit the manuscript.

292 **References**

- 293 1. Masoumi, M.: A highly efficient and secure hardware implementation of the advanced
294 encryption standard. *J. Inf. Secur. Appl.* **48**, 102371 (2019)
295 <https://doi.org/10.1016/j.jisa.2019.102371>
- 296 2. Chen, S., Yu, S., J, L., Chen, G., He, J.: Design and FPGA-based realization of a chaotic secure
297 video communication system. *IEEE Trans. Circuits Syst. Video Technol.* **28**(9), 2359-2371
298 (2018) <https://doi.org/10.1109/TCSVT.2017.2703946>
- 299 3. Wu, S., Li, Y., Li, W., Li, L.: Chaos criteria design based on modified sign functions with one
300 or three-threshold. *Chinese J. Electron.* **28**(2), 364-369 (2019)
301 <https://doi.org/10.1049/cje.2018.02.001>
- 302 4. Liu, X., Tong, X., Wang, Z., Zhang, M., Fan, Y.: A novel devaney chaotic map with uniform
303 trajectory for color image encryption. *Appl. Math. Model.* **120**, 153-174 (2023)
304 <https://doi.org/10.1016/j.apm.2023.03.038>
- 305 5. Elsadany, A.A., Hussein, S., Al-khedhairi, A., Elsonbaty, A.: On dynamics of 4-D blinking
306 chaotic system and voice encryption application. *Alex. Eng. J.* **70**, 701-718 (2023)
307 <https://doi.org/10.1016/j.aej.2023.03.024>
- 308 6. Zhou, S., Wang, X., Zhang, Y.: Novel image encryption scheme based on chaotic signals with
309 finite-precision error. *Inf. Sci.* **621**, 782-798 (2023) <https://doi.org/10.1016/j.ins.2022.11.104>
- 310 7. John, S., Kumar, S.N.: 2D Lorentz chaotic model coupled with logistic chaotic model for
311 medical image encryption: Towards ensuring security for teleradiology. *Procedia Comput. Sci.*
312 **218**, 918-926 (2023) <https://doi.org/10.1016/j.procs.2023.01.072>
- 313 8. Liang, B., Hu, C., Tian, Z., Wang, Q., Jian, C.: A 3D chaotic system with multi-transient
314 behavior and its application in image encryption. *Phys. A: Stat. Mech. Appl.* **616**, 128624

- 315 (2023) <https://doi.org/10.1016/j.physa.2023.128624>
- 316 9. Lai, Q., Chen, Z.: Grid-scroll memristive chaotic system with application to image encryption.
317 Chaos Solit. Fractals. **170**, 113341 (2023) <https://doi.org/10.1016/j.chaos.2023.113341>
- 318 10. Zhu, S., Deng, X., Zhang, W., Zhu, C.: Secure image encryption scheme based on a new robust
319 chaotic map and strong S-box. Math. Comput. Simul. **207**, 322-346 (2023)
320 <https://doi.org/10.1016/j.matcom.2022.12.025>
- 321 11. Sriram, B., Ghaffari, A., Rajagopal, K., Jafari, S., Tlelo-Cuautle, E.: A chaotic map with
322 trigonometric functions: Dynamical analysis and its application in image encryption based on
323 sparse representation and convolutional filters. Optik **273**, 170379 (2023)
324 <https://doi.org/10.1016/j.ijleo.2022.170379>
- 325 12. Liu, L., Wang, J.: A cluster of 1D quadratic chaotic map and its applications in image
326 encryption. Math. Comput. Simul. **204**, 89-114 (2023)
327 <https://doi.org/10.1016/j.matcom.2022.07.030>
- 328 13. Cao, W., Cai, H., Hua, Z.: n-Dimensional Chaotic Map with application in secure
329 communication. Chaos Solit. Fractals. **163**, 112519 (2022)
330 <https://doi.org/10.1016/j.chaos.2022.112519>
- 331 14. Shahna, K.U.: Novel chaos based cryptosystem using four-dimensional hyper chaotic map
332 with efficient permutation and substitution techniques. Chaos Solit. Fractals. **170**, 113383
333 (2023) <https://doi.org/10.1016/j.chaos.2023.113383>
- 334 15. Peng, Y., He, S., Sun, K.: A higher dimensional chaotic map with discrete memristor. Int. J.
335 Electron. Commun. **129**, 153539 (2021) <https://doi.org/10.1016/j.aeue.2020.153539>
- 336 16. Wang, L., Sun, K., Peng, Y., He, S.: Chaos and complexity in a fractional-order higher-
337 dimensional multicavity chaotic map. Chaos Solit. Fractals. **131**, 109488 (2020)

- 338 <https://doi.org/10.1016/j.chaos.2019.109488>
- 339 17. Boriratrith, S., Fuangfoo, P., Srithapon, C., Chatthaworn, R.: Adaptive meta-learning extreme
340 learning machine with golden eagle optimization and logistic map for forecasting the
341 incomplete data of solar irradiance. *Energy and AI*. **13**, 100243 (2023)
342 <https://doi.org/10.1016/j.egyai.2023.100243>
- 343 18. Si, Y., Liu, H., Chen, Y.: Constructing a 3D Exponential Hyperchaotic Map with Application
344 to PRNG. *Int. J. Bifurcat. Chaos*. **32**(7), 2250095 (2022)
345 <https://doi.org/10.1142/S021812742250095X>
- 346 19. Belazi, A., El-Latif, A.A.A.: A simple yet efficient S-box method based on chaotic sine map.
347 *Optik* **130**, 1438-1444 (2017) <https://doi.org/10.1016/j.ijleo.2016.11.152>
- 348 20. Briggs, K.: An improved method for estimating Liapunov exponents of chaotic time series.
349 *Phys. Lett. A*. **151**(1), 27-32 (1990) [https://doi.org/10.1016/0375-9601\(90\)90841-B](https://doi.org/10.1016/0375-9601(90)90841-B)
- 350 21. Li, D., Li, J., Di, X.: A novel exponential one-dimensional chaotic map enhancer and its
351 application in an image encryption scheme using modified ZigZag transform. *J. Inf. Secur.*
352 *Appl.* **69**, 103304 (2022) <https://doi.org/10.1016/j.jisa.2022.103304>
- 353 22. Liu, H., Kadir, A., Xu, C.: Cryptanalysis and constructing S-Box based on chaotic map and
354 backtracking. *Appl. Math. Comput.* **376**, 125153 (2020)
355 <https://doi.org/10.1016/j.amc.2020.125153>
- 356 23. Si, Y., Liu, H., Chen, Y.: Constructing keyed strong S-Box using an enhanced quadratic map.
357 *Int. J. Bifurcat. Chaos*. **31**(10), 2150146 (2021) <https://doi.org/10.1142/S0218127421501467>
- 358 24. Liu, H., Kadir, A., Xu, C.: Color image encryption with cipher feedback and coupling chaotic
359 map. *Int. J. Bifurcat. Chaos*. **30**(12), 2050173 (2020)
360 <https://doi.org/10.1142/S0218127420501734>

- 361 25. Liu, B., Xiang, H., Liu, L.: Reducing the dynamical degradation of digital chaotic maps with
362 time-delay linear feedback and parameter perturbation. *Math. Probl. Eng.* **2020**, 4926937
363 (2020) <https://doi.org/10.1155/2020/4926937>
- 364 26. Zhu, L., Jiang, D., Ni, J., Wang, X., Rong, X., Ahmad, M., Chen, Y.: A stable meaningful
365 image encryption scheme using the newly-designed 2D discrete fractional-order chaotic map
366 and Bayesian compressive sensing. *Signal Process.* **195**, 108489 (2022)
367 <https://doi.org/10.1016/j.sigpro.2022.108489>
- 368 27. Hua, Z., Li, J., Chen, Y., Yi, S.: Design and application of an S-box using complete Latin
369 square. *Nonlinear Dyn.* **104**(1), 807-825 (2021) <https://doi.org/10.1007/s11071-021-06308-3>
- 370 28. Li, L., Liu, J., Guo, Y., Liu, B.: A new S-box construction method meeting strict avalanche
371 criterion. *J. Inf. Secur. Appl.* **66**, 103135 (2022) <https://doi.org/10.1016/j.jisa.2022.103135>
- 372 29. Fang, M., Xu, K., Yang, T., Meng, F., Yu, C.: AES intermediate variables vulnerability
373 recognition based on side channel attacks. *Appl. Res. Comput.* **30**, 1536-1539 (2017)
- 374 30. Ma, S., Jin, C., Guan, J., Liu, S.: Improved differential attacks on the reduced-round SNOW-
375 V and SNOW-Vi stream cipher. *J. Inf. Secur. Appl.* **71**, 103379 (2022)
376 <https://doi.org/10.1016/j.jisa.2022.103379>
- 377